Idelalisib Rescues Natural Killer Cells from Monocyte-Induced Immunosuppression by Inhibiting NOX2-Derived Reactive Oxygen Species

Ali A. Akhiani[1], Alexander Hallner[1,2], Roberta Kiffin[1,2], Ebru Aydin[1,2], Olle Werlenius[2,3], Johan Aurelius[2,3], Anna Martner[1,2], Fredrik B. Thorén[2,4], and Kristoffer Hellstrand[1,2]

ABSTRACT

The phosphatidylinositol-4,5-bisphosphate-3 kinase-δ (PI3Kδ) inhibitor idelalisib, used alone or in combination with anti-CD20, is clinically efficacious in B-cell lymphoma and chronic lymphocytic leukemia (CLL) by promoting apoptosis of malignant B cells. PI3K regulates the formation of reactive oxygen species (ROS) by the myeloid NADPH oxidase NOX2, but the role of PI3Kδ in myeloid cell–induced immunosuppression is unexplored. We assessed the effects of idelalisib on the spontaneous and IgG antibody–induced ROS production by human monocytes, on ROS-induced cell death of human natural killer (NK) cells, and on tumor cell clearance in an NK cell–dependent mouse model of metastasis. Idelalisib potently and efficiently inhibited the formation of NOX2-derived ROS from monocytes and rescued NK cells from ROS-induced cell death. Idelalisib also promoted NK cell cytotoxicity against anti–CD20-coated primary human CLL cells and cultured malignant B cells. Experiments using multiple PI3K inhibitors implicated the PI3Kδ isoform in regulating NOX2-induced ROS formation and immunosuppression. In B6 mice, systemic treatment with idelalisib significantly reduced the formation of lung metastases from intravenously injected melanoma cells but did not affect metastasis in B6.129S6-Cybbtm1Din (*Nox2*$^{-/-}$) mice or in NK cell–deficient mice. Our results imply that idelalisib rescues NK cells from NOX2/ROS-dependent immunosuppression and thus exerts antineoplastic efficacy beyond B-cell inhibition.

Introduction

Chronic lymphocytic leukemia (CLL) is characterized by progressive clonal expansion of mature B lymphocytes (1). Therapy for CLL includes anti-CD20 IgG such as rituximab (RTX), ofatumumab (OFA), or glycoengineered obinutuzumab, which marks malignant cells for destruction by natural killer (NK) cells and myeloid cells (2, 3). NK cells and myeloid cells express Fc gamma receptors (FcγR) that attach the Fc portion of IgG to exert antibody-dependent cellular cytotoxicity (ADCC) or phagocytosis against foreign cells, including malignant B cells. ADCC exerted by NK cells has been proposed to contribute to the therapeutic efficacy of anti-CD20 in CLL and other B-cell malignancies (4–8). However, NK cells are dysfunctional in CLL (9–12), and patients may therefore benefit from therapies that augment NK cell survival and function.

Monocytes and other myeloid cells, including neutrophils, express the NOX2 isoform of NADPH oxidase, which generates reactive oxygen species (ROS). Exposure of monocytes and neutrophils to a variety of stimuli, including immobilized IgG antibodies, may activate NOX2 to generate ROS. Fc gamma receptor I (FcγRI, CD64), a high-affinity Fc receptor for IgG, is constitutively expressed by classical monocytes (CD14^{+}/CD16^{-}) and macrophages (13, 14). FcγRI cross-linking by IgG1 and IgG3 triggers intracellular signal transduction pathways that activates NOX2 to generate ROS (15, 16). Similarly, ligation of Fc gamma receptors (FcγRII, CD32 and FcγRIII, CD16) on the surface of monocytes and neutrophils by IgG can induce ROS production (17).

NOX2-derived ROS are pivotal for the elimination of ingested microbes (18) but may also be released extracellularly to suppress the function and viability of adjacent NK cells and T cells; these immunosuppressive properties comprise induction of PARP-dependent cell death characterized by nuclear accumulation of apoptosis-inducing factor and DNA degradation (19–23). Mice genetically deprived of NOX2 function (gp91$^{phox-/-}$ or *Nox2*$^{-/-}$) show improved NK cell–mediated clearance of metastatic cells but also develop autoimmunity, thus supporting the idea that NOX2-derived ROS may control NK cell and T-cell function *in vivo* (18, 24, 25).

The class I phosphatidylinositol 3 kinase (PI3K) produces the PIP3 lipid that is critical for activation of Akt (protein kinase B; ref. 26). Class I PI3Ks are heterodimeric enzymes that comprise a regulatory and a catalytic subunit. Class IA PI3Ks may contain the catalytic isoforms p110α, p110β, or p110δ, whereas p110γ is the single isoform of class IB PI3K. p110α and p110β are widely distributed in mammalian tissues, whereas p110δ is highly enriched in leukocytes (27, 28). The PI3Kδ-selective inhibitor idelalisib (CAL-101) inhibits PI3K targets in B-cell receptor signaling to promote apoptosis in CLL cells, supporting that PI3Kδ function is critical for CLL cell survival (29, 30). Idelalisib, alone or in conjunction with anti-CD20, is approved in Europe and the United States for use in CLL and other B-cell malignancies but is associated with several toxicities such as autoimmunity and severe infections, including opportunistic infections (31–36). Details

[1]Department of Infectious Diseases, Institute of Biomedicine, Sahlgrenska Academy, University of Gothenburg, Gothenburg, Sweden. [2]TIMM Laboratory, Sahlgrenska Center for Cancer Research, University of Gothenburg, Gothenburg, Sweden. [3]Department of Hematology, Institute of Medicine, Sahlgrenska Academy, University of Gothenburg, Gothenburg, Sweden. [4]Department of Medical Biochemistry and Cell Biology, Institute of Biomedicine, Sahlgrenska Academy, University of Gothenburg, Gothenburg, Sweden.

Note: Supplementary data for this article are available at Cancer Immunology Research Online (http://cancerimmunolres.aacrjournals.org/).

Corresponding Author: Kristoffer Hellstrand, Institute of Biomedicine, University of Gothenburg, Box 425, 40530 Gothenburg, Sweden. Phone: 46-31-786-6672; E-mail: kristoffer.hellstrand@microbio.gu.se

Cancer Immunol Res 2020;8:1532–41

doi: 10.1158/2326-6066.CIR-20-0055

regarding mechanisms underlying these toxicities and the benefit of the anti-CD20/idelalisib interaction are not known.

PI3K is implicated in regulation of NOX2-derived ROS formation in myeloid cells, including cells of the monocyte/macrophage lineage (37, 38). Akt phosphorylates the $p47^{phox}$ subunit of NOX2 (39) and thus contributes to the initiation of ROS production. Anti-CD20 triggers neutrophils and monocytes to release extracellular ROS that inhibit the survival and function of adjacent NK cells (10, 40).

Here, we assessed the role of PI3K, in particular PI3Kδ, in antibody-induced ROS formation and NK cell dysfunction. We observed that idelalisib prevented Akt-dependent phosphorylation of the $p47^{phox}$ subunit of NOX2, suppressing anti–CD20-induced ROS formation by human monocytes. Idelalisib rescued NK cells from ROS-induced toxicity and improved NK cell–mediated ADCC against primary and cultured malignant B cells. In mice, systemic treatment with idelalisib reduced hematogenous metastasis by a mechanism that required intact NOX2 and presence of NK cells. Our findings provide additional insight into the mechanisms of idelalisib efficacy and toxicity.

Materials and Methods

Compounds

The following compounds and reagents were used: RTX (Roche AB; Pharmacy catalog no. 494237), OFA (Novartis Pharmaceuticals Corporation; Pharmacy catalog no. 699855), cetuximab (Sigma-Aldrich; catalog no. MSQC18), the PI3Kδ inhibitor idelalisib (CAL101; Selleckchem; catalog no. S2226; ref. 30), the PI3Kβ inhibitor TGX-221 (Selleckchem; catalog no. S1169; ref. 37), the PI3Kα inhibitors HS-173 (ref. 41; Selleckchem; catalog no. S7356) and GDC-0326 (Selleckchem; catalog no. S8157; ref. 42), the PI3Kγ inhibitor AS-252424 (Selleckchem; catalog no. S2671; ref. 37), the pan-PI3K inhibitor LY294002 (Cell Signaling Technology; catalog no. 9901; ref. 43), the NOX2 inhibitor diphenylene iodonium (DPI; Sigma-Aldrich; catalog no. D2926; ref. 44), the ROS scavenger catalase (Worthington; catalog no. LS001872; ref. 45), DMSO (Sigma-Aldrich; catalog no. D2650–100ML; used for dissolving PI3K inhibitors and DPI), CellTrace violet stain (Thermo Fisher Scientific; catalog no. C34557), and anti–CD107a-PE-Cy7 Ab (BD Pharmingen; catalog no. 561348).

Isolation of leukocytes

Blood samples were collected from 6 patients with CLL. The patients provided written-informed consent, and the study was performed in accordance with the Declaration of Helsinki. Patients were asymptomatic, Binet stage A and did not undergo treatment for CLL (including chemotherapy, corticosteroids, anti-CD20, or other B-cell–inhibitory treatment) at the time of participation and sampling. Leukopacks from anonymized healthy blood donors were obtained from the Blood Center at Sahlgrenska University Hospital. Peripheral blood mononuclear cells (PBMC) from patients with CLL and healthy donors were isolated using dextran sedimentation followed by density gradient centrifugation using Lymphoprep (Alere Technologies AS; catalog no. 1114547; ref. 22). NK cells ($CD3^-/CD56^+$; Miltenyi Biotec; catalog no. 130–092–657) and monocytes ($CD14^+/CD16^-$) from healthy donors were enriched from PBMCs by immunomagnetic isolation using an MACS NK cell isolation kit and a MACS monocyte isolation kit II (Miltenyi Biotec; catalog no. 130–091–153), respectively, according to the manufacturer's instructions. In these experiments, the purity of isolated NK cells and monocytes exceeded 96% and 92%, respectively (Supplementary Fig. S1A and S1B). Primary CLL cells were isolated from patient PBMCs using the MACS B-cell (B-CLL) isolation kit according to the manufacturer's instructions (purity >90%; Miltenyi Biotec; catalog no. 130–093–660; Supplementary Fig. S1C). The enriched B cells from patients were resuspended in Iscove's modified Dulbecco minimum essential medium supplemented with 10% human AB+ serum and used as target cells in assays of ADCC as described below. The 221 B lymphoblastoid cell line (46) was kindly provided by Professor Alessandro Moretta, University of Genoa, Genoa, Italy, in 2016 and grown in RPMI 1640 medium with 10% FCS and 1% L-glutamine. The cells carried lymphoblastic morphology and stained with human anti-CD20 using flow cytometry but were otherwise not authenticated. The 221 cells were checked for absence of mycoplasma using PCR before freezing aliquots. Each aliquot was thawed and cultured for no more than 2 months for each experiment.

Cell death assays

NK cells and monocytes were cocultured in 96-well plates overnight at 37°C and 5% CO2 in the presence or absence of IgG isotype mAbs (10 μg/mL, RTX and OFA), with PI3K isoform–selective inhibitors (idelalisib, TGX-221, HS-173, GDC-0326, or AS-252424), the pan-PI3K inhibitor LY294002 (5 μmol/L), the NOX2 inhibitor DPI (3 μmol/L), the ROS scavenger catalase (200 U/mL), or DMSO (control), as indicated in figure legends. In some experiments, RTX and OFA Fab fragments (10 μg/mL; ref. 10) were used to define the role of the Fc portion. To determine the effect of antibody-independent ROS-induced cell death, NK cells were cocultured overnight with monocytes in 96-well low-adherence plates in the absence of antibodies. In this model, low-adherence plates favor cell–cell interactions and allow spontaneous ROS production from monocytes toward the NK cells. NK cell viability was assessed by flow cytometry (using a 4-laser BD LSR Fortessa and BD FACS Diva software, BD Biosciences) after staining with the Live/Dead Fixable Dead Cell Stain kit (Thermo Fisher Scientific; catalog no. L10120) according to the manufacturer's instructions. Cell death was measured as the percentage of the Live/Dead-positive cells and confirmed using the altered scatter characteristics displayed by dead lymphocytes, i.e., a reduced forward scatter and an increased side scatter signal (19).

Assays of NK cell degranulation and ADCC

To determine NK cell cytotoxicity against malignant B cells after exposure to ROS-producing monocytes, NK cells and monocytes were first cocultured in 96-well plates overnight with or without immobilized RTX (10 μg/mL) and in the presence or absence of idelalisib (0.1–0.2 μmol/L), LY294002 (5 μmol/L), or catalase (200 U/mL) using the diluent (sodium chloride or DMSO) as control. After 16 hours, CellTrace violet–labeled primary CLL cells or 221 B-lymphoblastoid cells coated with RTX (10 μg/mL) were added at an effector to target cell ratio of 2:1 (NK:CLL) together with anti–CD107a-PE-Cy7. After another 4 hours of incubation, plates were centrifuged at 500G for 5 minutes, the supernatant was discarded, and cells were stained with the Live/Dead Far Red Dead Cell Stain. Cell death in target cells and NK cells as well as NK cell degranulation was assayed by flow cytometry using the aforementioned anti-CD107a. Lysed primary CLL and 221 target cells were identified as Cell Trace violet–positive Live/Dead Far Red–positive cells. Dead NK cells were identified as Cell Trace violet–negative Live/Dead Far Red–positive cells (for gating strategy of lysed and dead cells, see Supplementary Fig. S1D and S1E). NK cell degranulation was estimated as the percentage of viable NK cells (gated as Live/Dead Far Red negative, non–Cell Trace violet-labeled cells within the FSC/SSC gate comprising lymphocytes) that stained positively for CD107a (47) using gating strategies as

previously described (48). In some experiments, NK cells were directly cocultured with RTX-coated primary CLL cells in the presence of monocytes for 4 hours followed by assay of ADCC and NK cell degranulation.

Measurement of ROS

ROS production from monocytes was measured by isoluminol-enhanced chemiluminescence that only captures extracellular ROS (21). In brief, 2×10^5 purified monocytes from healthy donors were added to 96-well plates in the presence of isoluminol (10 mg/mL) and horseradish peroxidase (HRP, 4 U/mL, Sigma-Aldrich; catalog no. 516531–25KU) and presence or absence of IgG isotype mAbs (RTX, OFA, or cetuximab) or Fab fragments, as indicated in figure legends. The release of extracellular ROS (light emission) was continuously monitored using a BMG FLUOStar Microplate Reader (BMG Labtech). ROS production (chemiluminescence) was calculated as the AUC. In some experiments, monocytes were stimulated with phorbol myristate acetate (PMA, 50 nmol/L, an activator of protein kinase C, Sigma-Aldrich; catalog no. P1585–1MG; ref. 49) and assayed for extracellular ROS production. In mouse experiments, $Gr1^+$ cells were isolated through magnetic separation from harvested bone marrow samples (50) followed by the isoluminol-based ROS production assay using the BMG FLUOStar Microplate Reader as described above.

H_2O_2 consumption assay

Consumption of hydrogen peroxide was determined as described (22, 51). In brief, compounds were diluted in Krebs–Ringer glucose (KRG) buffer and incubated with 50 μmol/L H_2O_2 for 15 minutes using catalase (200 U/mL) as the positive control. Remaining H_2O_2 was determined fluorimetrically by measurement of oxidation of p-hydroxyphenyl acetic acid (Sigma-Aldrich; catalog no. H50004; 0.5 mg/mL) catalyzed by HRP (4 U/mL), using the BMG FLUOStar Microplate Reader (excitation, 320 nm; emission 400 nm).

Western blot analysis of phosphorylated Akt and $p47^{phox}$

Cell lysates from monocytes were prepared as described (22). Briefly, monocytes were disrupted in RIPA buffer (Sigma-Aldrich; catalog no. R0278–50ML) containing a protease inhibitor cocktail (Sigma-Aldrich; catalog no. P8340). The protein concentration of the cell lysate was determined using the Pierce BCA protein assay kit (Thermo Fisher Scientific; catalog no. 23227). The lysate was mixed with NuPAGE LDS sample buffer (Invitrogen; catalog no. NP0007) and NuPAGE sample reducing agent (Invitrogen; catalog no. NP0004), heated at 70°C for 10 minutes, and resolved on 4%–12% NuPAGE Novex Bis-Tris precast gels (Invitrogen). After electrophoresis, proteins were transferred to nitrocellulose membranes using the iBlot Gel Transfer Device (Invitrogen). Membranes were blocked with buffered saline containing detergent and Hammersten casein solution (Invitrogen; catalog no. WB7050). For detection of phosphorylated Akt and $p47^{phox}$, membranes were incubated with a rabbit phospho-Akt (Ser473) polyclonal antibody (Cell Signaling Technology; catalog. no. 9271; 1:1,000) or with a rabbit phospho-$p47^{phox}$ (Ser304) polyclonal antibody (Abcam; catalog no. ab63554; 1:500), respectively, followed by incubation with an HRP-conjugated goat anti-rabbit (DAKO; catalog no. P0448; 1:1,000). Bound antibodies were visualized by enhanced chemiluminescence (Chemi-Doc, Bio-Rad) with Clarity Western ECL Substrate (Bio-Rad; catalog no. 1705060). Band intensity was quantified using the NIH ImageJ software (52). The nitrocellulose membranes were then stripped with NewBlot IR Stripping buffer (LI-COR; catalog no. 928–40028) for 15 minutes at room temperature and reprobed with rabbit anti total-$p47^{phox}$ (Cell Signaling Technology; catalog no. 4312; 1:1,000) or with rabbit GAPDH (D16H11) monoclonal antibody (Cell Signaling Technology; catalog no. 5174; 1:1,000). Cell lysate content of GAPDH was used as the loading control.

Generation of F_{ab2} fragments

F_{ab2} fragments of RTX and OFA were generated as previously described (10). Briefly, these Fab fragments were prepared by pepsin digestion using the Pierce F(ab)2 preparation kit (Thermo Fisher Scientific; catalog no. 44988) according to the manufacturer's instructions. Digestion and purity were confirmed by SDS-PAGE gel.

In vivo metastasis model

C57BL/6 mice were obtained from Charles River Laboratories, and B6.129S6-*Cybb*^{tm1Din} (*Nox2*$^{-/-}$ or *Nox2*-KO) mice, which lack functional ROS-forming NOX2 (25), were obtained from The Jackson Laboratory. The wild-type (WT) and *Nox2*-KO mice were kept under pathogen-free conditions according to guidelines issued by the University of Gothenburg. B16F10 cells were confirmed by use of PCR to be of mouse origin, and no mammalian interspecies contamination was detected (Idexx Bioanalytics). The B16F10 cells showed minor genetic changes (addition of an allele at marker MCA-5–5), but were otherwise identical to the genetic profile established for this cell line (Idexx Bioanalytics). The B16F10 cells were checked for absence of mycoplasma using PCR before freezing aliquots and were cultured in Iscove's medium containing 10% FCS (Sigma-Aldrich), 2 mmol/L L-glutamine, 1 mmol/L sodium pyruvate, 100 U/mL penicillin, and 100 mg/mL streptomycin at 37°C for 1 week prior to start of experiments. Genetic depletion of *Nox2* entails reduced B16F10 metastasis (18, 25). To achieve comparable numbers of metastases, we injected 10×10^4 B1610 cells in 0.1 mL KRG intravenously (tail vein injection) per WT mouse and 15×10^4 cells in 0.1 mL per *Nox2*-KO mouse. After B16F10 cell injection, mice were treated i.p. with idelalisib (40 mg/kg in 0.1 mL diluted in DMSO) or vehicle (control) for 5 consecutive days. Three weeks after tumor injection, mice were euthanized, and visible pulmonary metastatic foci were enumerated by light microscopy. In NK depletion experiments, mice were injected i.p. with 250 μg NK1.1 ab (Invivomab in 0.1 mL) 1 day prior to inoculation as described (25). This procedure depleted >95% of $NK1.1^+$ cells (out of all $CD45^+$ cells) from peripheral blood for at least 6 days (Supplementary Fig. S1F).

Statistical analyses and ethical considerations

One-way ANOVA followed by Bonferroni's correction was used for multiple comparisons, Student *t* test was used in all figures, and asterisks are used as follows: *, $P < 0.05$; **, $P < 0.01$; ***, $P < 0.001$; and ****, $P < 0.0001$. All indicated *P* values are two-sided. The study was approved by the Ethical Review Board of Gothenburg (application no. 312-13), and all experiments were performed in accordance with the Declaration of Helsinki. Animal experiments were approved by the Research Animal Ethics Committee at the University of Gothenburg, Sweden (application no. 86-14).

Results

Idelalisib inhibited phosphorylation of NOX2/p47 and antibody-induced ROS

PI3K is implicated in the regulation of NOX2-derived ROS formation in myeloid cells, but the role of PI3K isoforms in NOX2 regulation

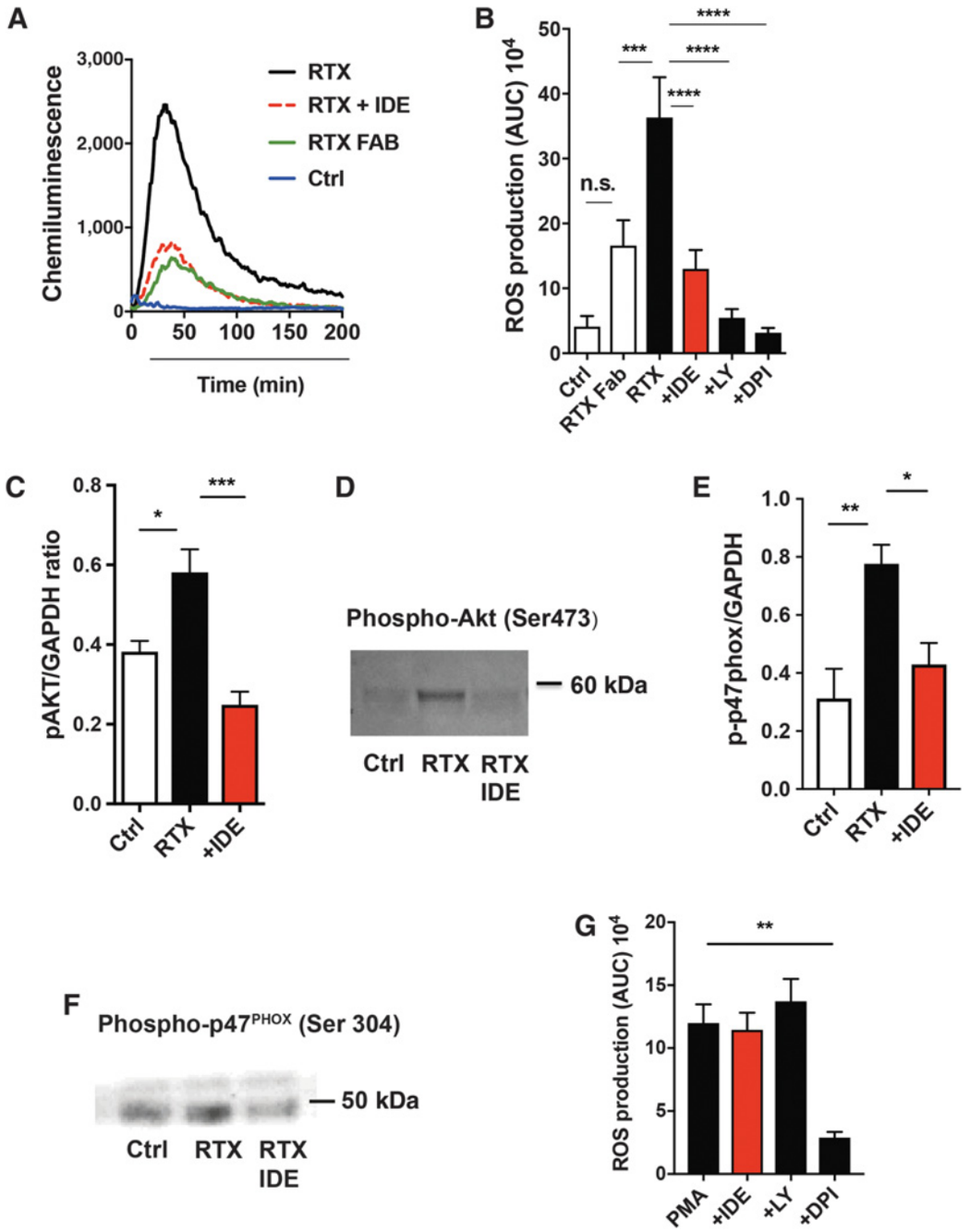

Figure 1.

Idelalisib suppressed ROS formation in antibody-stimulated monocytes by targeting Akt-dependent p47^{phox} phosphorylation. **A** and **B,** Purified monocytes were continuously assessed for extracellular ROS production by chemiluminescence in the presence of plate-bound RTX (10 μg/mL) or RTX Fab fragment (RTX FAB; 10 μg/mL) and presence of the PI3Kδ inhibitor idelalisib (IDE; 0.1 μmol/L), the pan-PI3K inhibitor LY294002 (LY; 5 μmol/L), the NADPH inhibitor DPI (3 μmol/L), or DMSO (Ctrl). Representative ROS measurement (chemiluminescence; **A**) and total monocyte ROS production (AUC), mean ± SEM of 7 donors (**B**) are shown. **C–F,** Monocytes were stimulated with plate-bound RTX (100 μg/mL) in the presence or absence of IDE (0.4 μmol/L) for 30 minutes or left unstimulated on ice for 30 minutes. Cells were then lysed and assayed for AKT (**C** and **D**) and p47^{phox} (**E** and **F**) phosphorylation by Western blot. Data shown (optical density) in **C** and **E** are mean ± SEM of results from 4 donors. GAPDH was used as loading control. Representative Western blots of phospho-AKT and phospho-p47^{phox} are shown in **D** and **F**, respectively. **G,** Extracellular ROS production from monocytes was measured by chemiluminescence in the presence of PMA (50 nmol/L) and presence of the PI3Kδ inhibitor IDE (0.1 μmol/L), the pan-PI3K inhibitor LY (5 μmol/L), or the NOX2 inhibitor DPI (3 μmol/L). Data shown are mean ± SEM of 4 donors. n.s., not significant; *, $P < 0.05$; **, $P < 0.01$; ***, $P < 0.001$; and ****, $P < 0.0001$ (one-way ANOVA followed by Bonferroni's correction).

is incompletely understood (37, 38). In agreement with a previous publication (10), immobilized RTX but not RTX F_{ab} fragments triggered robust ROS production from human monocytes (**Fig. 1A** and **B**). This implies that these cells are induced to generate ROS by binding to the F_c-part of anti-CD20. The PI3K p110δ inhibitor idelalisib inhibited RTX-induced formation of extracellular ROS by monocytes (**Fig. 1A** and **B**). Dose-response analysis suggested that idelalisib inhibited RTX-induced ROS formation with an IC_{50} of approximately 25 nmol/L (Supplementary Fig. S2A). The pan-PI3K inhibitor LY294002 and the NOX2 inhibitor DPI (**Fig. 1B**) exerted similar inhibition of anti–CD20-induced ROS formation.

We next defined a putative link between the PI3Kδ and NOX2 intracellular transduction pathways. Akt is a downstream target of PI3K that may activate NOX2 by phosphorylating Ser304 and Ser328 of the cytosolic subunit $p47^{phox}$ (39). To determine the involvement of PI3Kδ in anti–CD20-induced NOX2 activation, human monocytes were stimulated with RTX in the presence or absence of idelalisib to assay Akt and $p47^{phox}$ phosphorylation by Western blot. **Figure 1C–F** show RTX-induced phosphorylation of Akt at Ser473 and $p47^{phox}$ at Ser304 in monocytes. The antibody-induced $p47^{phox}$ phosphorylation was inhibited by idelalisib; as expected, idelalisib did not inhibit extracellular ROS production induced by PMA, which directly activates protein kinase C (**Fig. 1G**).

Idelalisib rescued NK cells from ROS-induced cell death

By releasing ROS, monocytes have been reported to trigger cell death by parthanatos in adjacent antineoplastic lymphocytes (23). Subsets of NK cells ($CD56^{dim}/CD16^{+}$ "cytotoxic" NK cells) are particularly sensitive to ROS-induced immunosuppression and death, presumably because $CD56^{dim}/CD16^{+}$ NK cells contain low levels of intracellular ROS-protective thiols (53). We determined whether CD20 antibodies affected NK cell viability in monocyte/NK cell cocultures and whether PI3K inhibitors prevented NK cell death. The addition of immobilized RTX triggered extensive NK cell death after overnight incubation with monocytes (**Fig. 2A**). NK cell death was prevented by the pan-PI3K inhibitor LY294002, the NOX2 inhibitor DPI, and the ROS scavenger catalase, implying that PI3K and NOX2 mediated cell death. Notably, no substantial increase in NK cell death was observed after overnight culture of NK cells with immobilized RTX in the absence of monocytes.

Monocytes from healthy subjects predominantly express the p110δ (class IB) isoform of PI3K but may also express α, β, and γ (class IA) isoforms (Supplementary Fig. S2B). Supplementary Table S1 shows the previously reported IC_{50}s (in cell-free experiments) of isoform-selective class I PI3K inhibitors. To determine effects of the PI3K inhibitors on ROS production and NK cell death triggered by RTX, we used each inhibitor at its reported IC_{50} value. **Figure 2B** shows a representative experiment of the effects of PI3K inhibitors on RTX-induced ROS production from monocytes, and **Fig. 2C** shows boxplots summarizing results achieved in six donors. In these experiments, idelalisib consistently reduced or inhibited RTX-induced ROS formation, whereas α and γ inhibitors did not. The p110β inhibitor TGX-221 tended to inhibit ROS formation ($P = 0.07$; **Fig. 2B** and **C**), which may be explained by the earlier reported affinity of TGX-221 for p110δ at higher concentrations (Supplementary Table S1). Effects of PI3K inhibitors on NK cell death largely mirrored those observed in assays of RTX-induced ROS formation. Hence, idelalisib prevented NK cell death with an IC_{50} of approximately 25 nmol/L, which was partly mimicked by a p110β inhibitor but not by α or γ inhibitors (**Fig. 2D**; Supplementary Fig. S2D). None of the PI3K inhibitors displayed ROS-scavenging properties, thus supporting that effects on ROS production resulted from the targeting of NOX2 (Supplementary Fig. S3).

OFA, a humanized antibody against CD20 (54), shared the property of RTX to induce ROS production from monocytes in an idelalisib-reversible fashion (Supplementary Fig. S4A and S4B). Idelalisib also prevented the ROS-dependent NK cell death induced by OFA (Supplementary Fig. S5A and S5B). In addition, the IgG1 antibody cetuximab (directed against the EGFR; ref. 55) efficiently triggered idelalisib-reversible ROS production from monocytes (Supplementary Fig. S2C), thus implying that IgG-induced ROS formation occurred independently of antigen specificity.

Next, we addressed the ability of idelalisib to restore NK cell cytotoxic responses. Freshly isolated NK cells were cocultured with RTX-coated primary CLL cells in the presence or absence of monocytes. After 4 hours, we determined the percentage of degranulating $CD107^{+}$ NK cells in the culture (48) and determined the proportion of lysed CLL cells. As shown in **Fig. 3A** and **B**, idelalisib partially prevented loss of ADCC and degranulation responses in ROS-exposed NK cells. No substantial induction of NK cell death was observed in these short assays (Supplementary Fig. S6F). In a next series of experiments, we asked if NK cells that had been rescued from ROS-induced death by idelalisib remained functional in terms of cytotoxicity against malignant B cells. We therefore generated cocultures of NK cells and monocytes and added immobilized RTX and idelalisib followed by assay of NK cell–mediated ADCC, using anti-CD20 as the linking antibody. NK cells rescued from ROS-mediated cell death by idelalisib or other ROS inhibitors (Supplementary Fig. S6A) remained functional and exerted ADCC and degranulation against 221 cells (**Fig. 3C** and **D**). Similar results were obtained using ADCC experiments with primary CLL cells as target cells (**Fig. 3E** and **F**; gating strategy and representative FACS plots are shown in Supplementary Fig. S1D and S1E). Effects of idelalisib on NK cell degranulation and ADCC were mimicked by the pan-PI3K inhibitor Ly294002 and the ROS scavenger catalase (**Fig. 3C–F**). Exposure of NK cells to idelalisib in the absence of monocytes in the overnight culture did not affect their ADCC against RTX-coated primary CLL cells or 221 cells (Supplementary Fig. S6B and S6C). Incubation of NK cells with RTX in the absence of monocytes in the overnight culture did not significantly affect NK cell viability (Supplementary Fig. S6D). Monocytes triggered only minor RTX-dependent ADCC against CLL cells (Supplementary Fig. S6E). Collectively, these results implied that idelalisib exerted potent NOX inhibition while protecting NK cells against ROS-induced inactivation.

Idelalisib inhibited ROS production and reduced B16F10 melanoma metastasis

We asked if idelalisib may also prevent myeloid cell–mediated immunosuppression in the absence of ROS-inducing antibodies or other NOX2 stimuli. We first observed that idelalisib inhibited the constitutive ROS production by unstimulated human monocytes (Supplementary Fig. S7A–S7C). Next, NK cells were cocultured overnight with monocytes (in the absence of antibodies) followed by assay of ADCC against primary human CLL cells. Idelalisib prevented NK cell death in these experiments (Supplementary Fig. S7D) and maintained NK cell cytotoxicity against primary CLL cells (Supplementary Fig. S7E and S7F), thus suggesting that idelalisib preserved NK cell function and viability also in the absence of exogenous antibodies.

We used genetically *Nox2*-deficient and NK cell–depleted mice to determine if the NOX2-inhibitory properties of idelalisib translated into improved NK cell–mediated clearance of malignant cells *in vivo*. Pharmacologic or genetic inhibition of NOX2 reduces lung metastasis

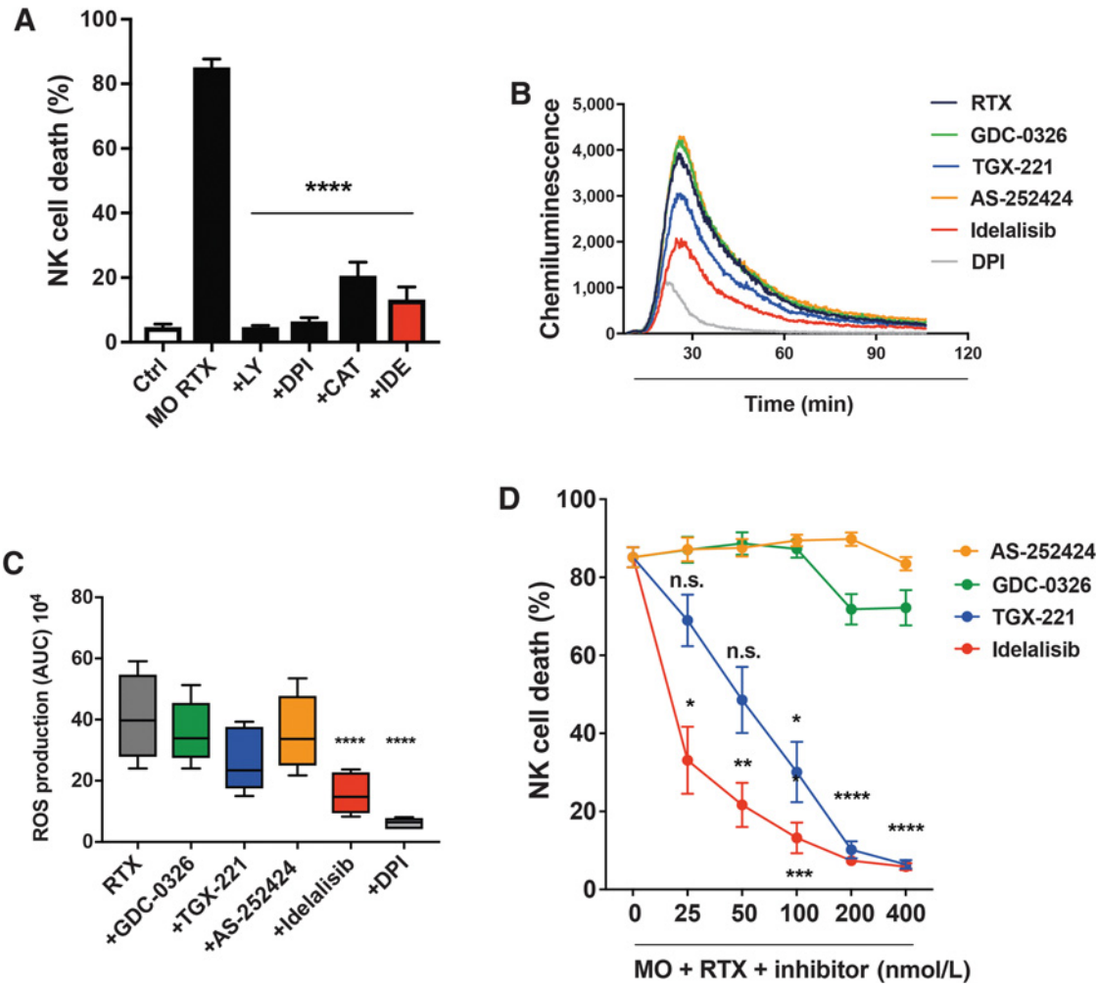

Figure 2.

Idelalisib rescued NK cells from cell death induced by CD20 antibodies. **A,** Human NK cells were incubated overnight with monocytes (MO) at a 2:1 ratio in the presence of plate-bound RTX (10 μg/mL) and the pan-PI3K inhibitor LY294002 (LY; 5 μmol/L), the NOX2 inhibitor DPI (3 μmol/L), the ROS scavenger catalase (CAT; 200 U/mL), or idelalisib (IDE; 0.1 μmol/L). The bars show mean NK cell death and are the mean ± SEM of five independent experiments. NK cells incubated with medium alone served as control (Ctrl). **B** and **C,** Human monocytes were assayed for extracellular ROS production by chemiluminescence in RTX-coated wells in the presence of PI3K isoform–selective inhibitors (the α inhibitor GDC-0326, the β inhibitor TGX-221, the γ inhibitor AS-252424, or the δ inhibitor IDE). **B** shows a representative ROS measurement (chemiluminescence) from monocytes using each PI3K inhibitor at 5 times the reported IC_{50} value (α—1 nmol/L, β—35 nmol/L, γ—175 nmol/L, or δ—12.5 nmol/L). **C** shows box-and-whiskers plots of the total monocyte ROS production (AUC). Results were obtained in six independent experiments. **D** shows anti-CD20-induced NK cell death using the same experimental setup as in **A** and compares NK cell protective properties of the PI3K-selective inhibitors at indicated final concentrations. Results show the mean ± SEM of results obtained in five independent experiments. n.s., not significant; *, $P < 0.05$; **, $P < 0.01$; ***, $P < 0.001$; and ****, $P < 0.0001$ (one-way ANOVA followed by Bonferroni's correction).

from B16F10 melanoma cells in mice; in this model, NK cells are significant mediators of tumor cell clearance (25). *Ex vivo* experiments verified that idelalisib inhibited constitutive ROS production by unstimulated murine myeloid $Gr1^+$ cells (B6 strain; **Fig. 4A**). $Gr1^+$ cells from *Nox2*-KO mice have no detectable ROS production by chemiluminescence (25). To assess effects of idelalisib on B16F10 metastasis, B6 mice were inoculated i.v. with B16F10 cells and treated with idelalisib (40 mg/kg x V) or vehicle followed by enumeration of melanoma metastases in lungs 3 weeks later (**Fig. 4B**). We observed significantly reduced melanoma metastasis in the idelalisib-treated WT mice. This effect was absent in *Nox2*-KO mice and in NK cell–depleted mice (**Fig. 4C–E**; Supplementary Fig. S1F), suggesting that the antimetastatic properties of idelalisib were NK cell–dependent and resulted from regulation of NOX2.

Discussion

Idelalisib is used in conjunction with RTX in patients with B-CLL and B cell lymphoma. Idelalisib inhibits PI3K targets in BCR signaling to promote apoptosis of malignant B cells (30). Here, we presented results suggesting a supplementary antineoplastic mechanism for idelalisib, where it prevents Akt-dependent phosphorylation of the NOX2 component $p47^{phox}$ in human myeloid cells and blocks the formation and release of immunosuppressive ROS, thus improving NK cell survival and cytotoxicity against leukemic cell lines and

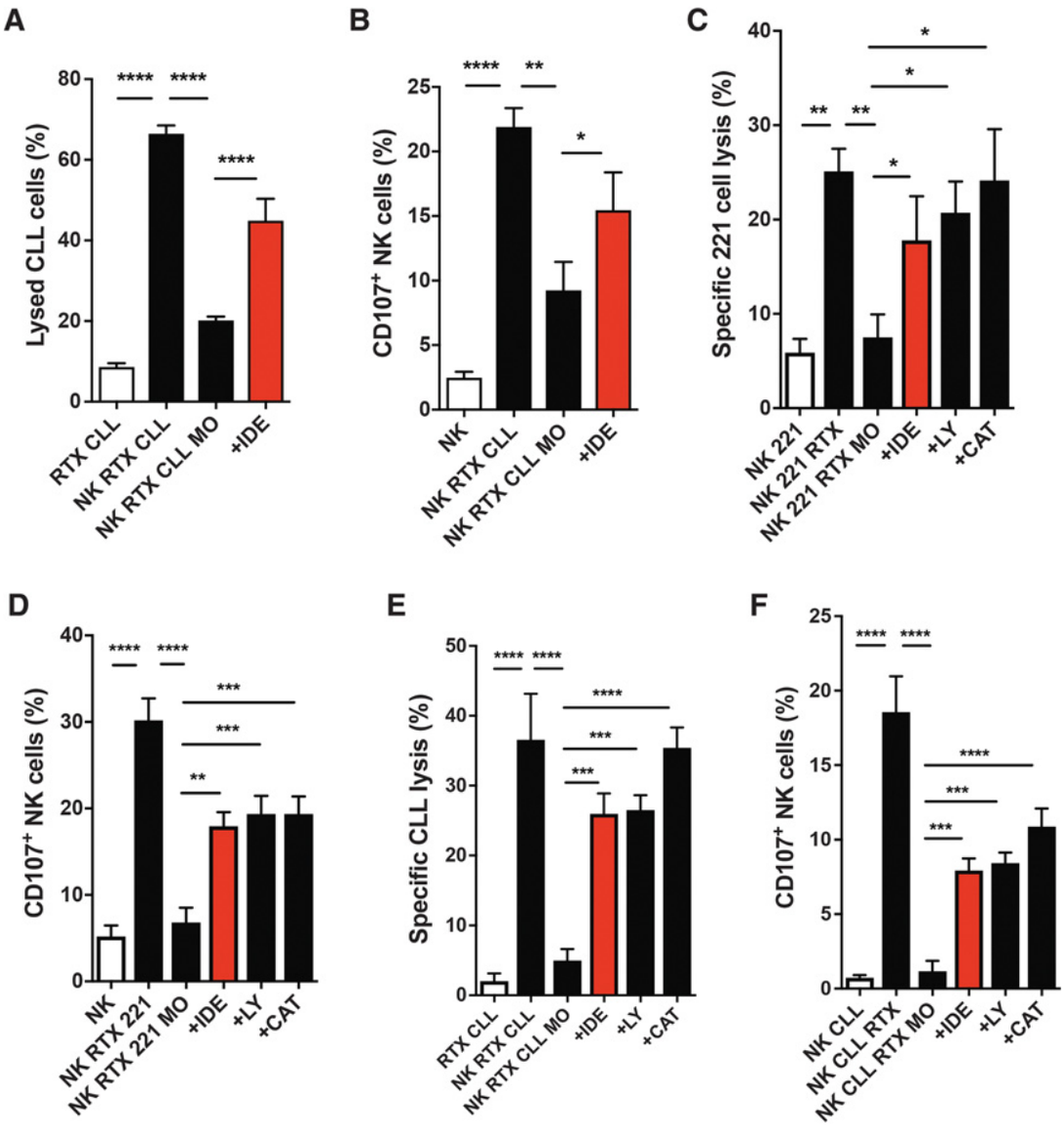

Figure 3.

NK cells rescued by idelalisib (IDE) from antibody-induced ROS toxicity retained ADCC against primary and cultured malignant B cells. **A** and **B,** NK cells, monocytes (MO), and primary CLL cells (coated with RTX at 10 μg/mL and labeled with Cell Trace) were cocultured at a 4:2:1 ratio (NK:MO:CLL) together with anti-CD107a in the presence of IDE (0.1 μmol/L). After 4 hours, cell viability was assessed using the Live/Dead Far Red Cell Stain kit, and NK cell degranulation was measured by the expression of CD107a. Data shown are mean ± SEM ($n = 5$ donors analyzed in independent experiments). **C–F,** NK cells were incubated overnight with monocytes at a 2:1 ratio in the presence of plate-bound RTX (10 μg/mL) and presence of IDE (0.1 μmol/L), LY294002 (LY; 5 μmol/L), catalase (CAT; 200 U/mL), or DMSO. Note that 221 B lymphoblastoid cells (**C** and **D**; $n = 4$–5 donors) or primary CLL cells (**E** and **F**; $n = 6$) coated with RTX (10 μg/mL) and labeled with Cell Trace were subsequently added at an effector-to-target cell ratio of 2:1 (NK:CLL) together with anti-CD107a antibodies. After another 4 hours of incubation, cell viability and NK cell degranulation were measured as described above. Note that 221 cell lysis (**C**), primary CLL lysis (**E**), and NK degranulation (**D** and **F**) are shown (mean ± SEM). *, $P < 0.05$; **, $P < 0.01$; ***, $P < 0.001$; and ****, $P < 0.0001$ (one-way ANOVA followed by Bonferroni's correction).

primary leukemic cells. Studies in experimental animals showed that idelalisib reduced ROS formation from Gr1$^+$ cells and improved NK cell–dependent clearance of metastatic cells in WT mice but not in mice genetically deficient of *Nox2*. These data imply that idelalisib may exert antineoplastic effects *in vivo* by targeting NOX2. Notably, higher doses of idelalisib were required to inhibit ROS production from murine Gr1$^+$ cells *in vitro* compared with human monocytes. This may imply that human monocytes are more sensitive to idelalisib than their murine counterparts.

Our study aimed at defining the interplay between PI3K and NOX2 that leads to NOX2 activation and subsequent ROS production. Exposure of phagocytes to any of a variety of stimuli, including immobilized IgG antibodies, may activate the enzyme to generate large amounts of extracellular superoxide anion. A pivotal aspect of

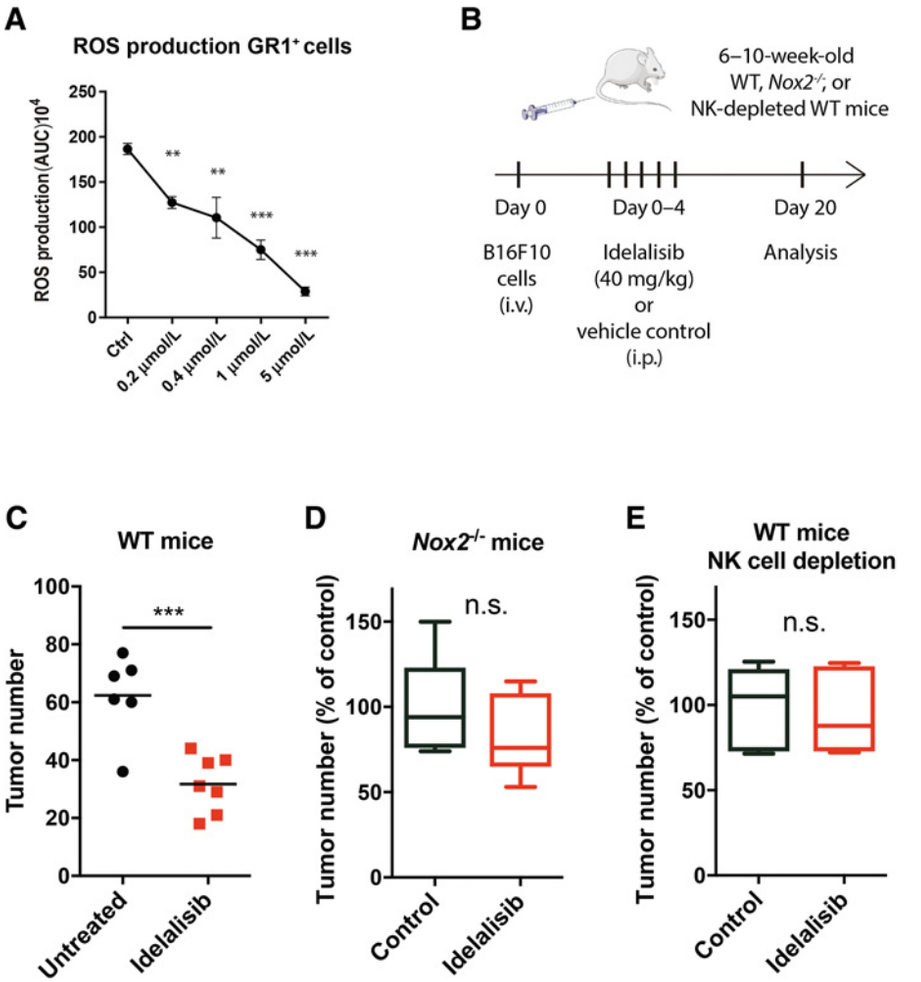

Figure 4.

Idelalisib inhibited ROS production from mouse Gr1$^+$ cells and promoted antimetastatic properties of NK cells *in vivo*. **A,** The constitutive ROS production (mean ± SEM) from murine BM Gr1$^+$ cells (recovered from 3 B6 WT mice in independent experiments) was assessed by chemiluminescence in the presence of DMSO (Ctrl) or idelalisib (0.2–5 μmol/L). **B,** The experimental design of the B16F10 metastasis model. The number of B16F10 lung metastases in mice 20 days after tail vein injection in WT B6 mice (**C**; control $n = 7$ mice, idelalisib $n = 7$), NOX2-deficient mice (**D**; control $n = 7$ mice, idelalisib $n = 7$), or NK cell–depleted B6 mice (**E**; control $n = 6$ mice, idelalisib $n = 6$). For each experiment and condition, the number of tumors in untreated control mice was normalized to 100%. All mice were treated with 40 mg/kg of idelalisib or vehicle (control) with a total of 5 i.p. injections. n.s., not significant; **, $P < 0.01$; and ***, $P < 0.001$ (Student *t* test).

NOX2 activation is the phosphorylation of the cytosolic subunit p47^{phox} (56, 57). Monocytes from patients with p47^{phox}-deficient chronic granulomatous disease (CGD) do not generate ROS via NOX2 and are therefore highly susceptible to bacterial infections. Patients with CGD are also prone to develop autoimmunity, presumably as a consequence of deficient ROS-mediated inactivation of lymphocyte-mediated autoimmunity (18, 58). There is an established role for PKC in p47^{phox} phosphorylation (56, 59, 60), but studies using PI3K inhibitors imply that the PI3K pathway also activates NOX2 (61, 62). We observed significant phosphorylation of Akt at Ser473 and p47^{phox} at Ser304 in monocytes shortly after stimulation with RTX, which was significantly inhibited by idelalisib. The Akt and p47^{phox} phosphorylation coincided with peak ROS production in stimulated monocytes, thus supporting the involvement of the PI3K–AKT pathway in antibody-induced NOX2 activation.

The role of PI3K isoforms in regulating NOX2-derived ROS has remained unknown. We used structurally distinct isoform-specific inhibitors of class I PI3K (Supplementary Table S1; Supplementary Fig. S8) and found that inhibition of the p110δ isoform using idelalisib efficiently blocked RTX-induced ROS production by human monocytes, whereas inhibitors of other isoforms exerted minor (p110β) or no (p110α and p110γ) effects on ROS production. Corresponding results were obtained in studies of protection of NK cells from ROS-induced cell death. These findings support that idelalisib primarily acts by blocking p110δ in reducing ROS formation and protecting NK cells. However, the potency and specificity of PI3K inhibitors may be context-dependent, and our results do not formally exclude that inhibition of isoforms of class I PI3K other than p110δ may have contributed to the observed ROS-inhibitory and immunostimulatory effects of idelalisib.

Our data suggest a mechanism by which idelalisib may restore NK cell function in an environment of NOX2-mediated oxidative stress. Although this study was focused on protection of NK cells against NOX2-derived ROS, subsets of T cells are sensitive to this mechanism of immunosuppression (63). In this context, global genetic depletion of the p110δ PI3K in mice impedes the development of murine CLL by restoring T-cell–mediated immunity (64). Further studies are required to determine if idelalisib, or other PI3Kδ inhibitors, may promote T-cell–mediated antitumor immunity by reducing NOX2-induced immunosuppression.

Our findings may be relevant beyond B-cell malignancies. For example, NOX2-dependent immunosuppression occurs in acute myeloid leukemia (21, 65). p110δ inhibitors are also effective in non-hematopoietic cancer. Thus, genetic or pharmacologic inactivation of p110δ was proposed to target the function of regulatory T cells, thus unleashing antitumor responses in experimental solid cancer (66). Using an *in vivo* melanoma model, we observed that inactivation of p110δ by idelalisib significantly reduced B16 lung metastasis

formation in an NK cell–dependent and NOX2-dependent manner. These results thus support that pharmacologic inhibition of p110δ may be useful in nonhematopoietic cancer (66) and imply that idelalisib may exert antineoplastic efficacy by preventing NOX2-mediated immunosuppression.

Patients treated with idelalisib are at risk for several toxicities such as autoimmunity and severe infections, including opportunistic infections (31–36). Reduced NOX2 function (in human CGD and in *Nox2*$^{-/-}$ mice) makes patients susceptible to microbial infections and autoimmunity (18). It may thus be speculated that the NOX2-inhibitory properties of idelalisib contribute to these toxicities. Notably, idelalisib reduced ROS formation from monocytes at concentrations similar to those detected in blood of idelalisib-treated patients (34), thus implying that idelalisib therapy is likely associated with significant NOX2 inhibition.

This study suggests an antineoplastic mechanism for PI3K p110δ blockade beyond interference with BCR signaling in malignant B cells. By targeting the p110δ/Akt signal transduction pathway that drives NOX2-dependent release of immunosuppressive ROS from myeloid cells, p110δ inhibitors may exert activity in a broader range of malignancies than previously appreciated.

Disclosure of Potential Conflicts of Interest

A. Martner and K. Hellstrand are authors of patents PCT/US2019/064151, PCT/US2019/045161, PCT/US2018/043693, and PCT/US2018/043543. A. Martner, F.B. Thorén, and K. Hellstrand are authors of patents PCT/US2019/038172 and WO2017137989A4. J. Aurelius, A. Martner, F.B. Thorén, and K. Hellstrand are authors of patent PCT/2018/040037. No potential conflicts of interest were disclosed by the other authors.

Authors' Contributions

A.A. Akhiani: Conceptualization, data curation, validation, investigation, methodology, writing–original draft, project administration, writing–review and editing. **A. Hallner:** Conceptualization, investigation, methodology, writing–original draft. **R. Kiffin:** Methodology. **E. Aydin:** Methodology. **O. Werlenius:** Data curation, methodology. **J. Aurelius:** Supervision. **A. Martner:** Conceptualization, resources, supervision, methodology. **F.B. Thorén:** Conceptualization, resources, formal analysis, supervision, investigation, methodology, writing–original draft, project administration, writing–review and editing. **K. Hellstrand:** Conceptualization, resources, data curation, supervision, funding acquisition, investigation, writing–original draft, project administration, writing–review and editing.

Acknowledgments

This work was supported by the Swedish Research Council, the Swedish Cancer Society, the Swedish state via the ALF agreement, the IngaBritt and Arne Lundberg Research Foundation, the Clas Groschinsky Foundation, the Åke Wiberg Foundation, the Assar Gabrielsson Foundation, the Lions Cancer Foundation West, the Wilhelm and Martina Lundgren Research Foundation, and BioCARE.

The costs of publication of this article were defrayed in part by the payment of page charges. This article must therefore be hereby marked *advertisement* in accordance with 18 U.S.C. Section 1734 solely to indicate this fact.

Received January 30, 2020; revised June 24, 2020; accepted September 16, 2020; published first September 23, 2020.

References

1. Rai KR, Jain P. Chronic lymphocytic leukemia (CLL)-then and now. Am J Hematol 2016;91:330–40.
2. Hallek M. Chronic lymphocytic leukemia: 2015 update on diagnosis, risk stratification, and treatment. Am J Hematol 2015;90:446–60.
3. Nabhan C, Rosen ST. Chronic lymphocytic leukemia: a clinical review. JAMA 2014;312:2265–76.
4. Dall'Ozzo S, Tartas S, Paintaud G, Cartron G, Colombat P, Bardos P, et al. Rituximab-dependent cytotoxicity by natural killer cells: influence of FCGR3A polymorphism on the concentration-effect relationship. Cancer Res 2004;64:4664–9.
5. Hatjiharissi E, Xu L, Santos DD, Hunter ZR, Ciccarelli BT, Verselis S, et al. Increased natural killer cell expression of CD16, augmented binding and ADCC activity to rituximab among individuals expressing the FcγRIIIa-158 V/V and V/F polymorphism. Blood 2007;110:2561–4.
6. Boross P, Jansen JH, de Haij S, Beurskens FJ, van der Poel CE, Bevaart L, et al. The in vivo mechanism of action of CD20 monoclonal antibodies depends on local tumor burden. Haematologica 2011;96:1822–30.
7. Cartron G, Dacheux L, Salles G, Solal-Celigny P, Bardos P, Colombat P, et al. Therapeutic activity of humanized anti-CD20 monoclonal antibody and polymorphism in IgG Fc receptor FcgammaRIIIa gene. Blood 2002;99:754–8.
8. Weng WK, Negrin RS, Lavori P, Horning SJ. Immunoglobulin G Fc receptor FcγRIIIa 158 V/F polymorphism correlates with rituximab-induced neutropenia after autologous transplantation in patients with non-Hodgkin's lymphoma. J Clin Oncol 2010;28:279–84.
9. Buechele C, Baessler T, Wirths S, Schmohl JU, Schmiedel BJ, Salih HR. Glucocorticoid-induced TNFR-related protein (GITR) ligand modulates cytokine release and NK cell reactivity in chronic lymphocytic leukemia (CLL). Leukemia 2012;26:991–1000.
10. Werlenius O, Aurelius J, Hallner A, Akhiani AA, Simpanen M, Martner A, et al. Reactive oxygen species induced by therapeutic CD20 antibodies inhibit natural killer cell-mediated antibody-dependent cellular cytotoxicity against primary CLL cells. Oncotarget 2016;7:32046–53.
11. Katrinakis G, Kyriakou D, Papadaki H, Kalokyri I, Markidou F Eliopoulos GD. Defective natural killer cell activity in B-cell chronic lymphocytic leukaemia is associated with impaired release of natural killer cytotoxic factor(s) but not of tumour necrosis factor-alpha. Acta Haematol 1996;96:16–23.
12. Kay NE, Zarling JM. Impaired natural killer activity in patients with chronic lymphocytic leukemia is associated with a deficiency of azurophilic cytoplasmic granules in putative NK cells. Blood 1984;63:305–9.
13. Dai X, Jayapal M, Tay HK, Reghunathan R, Lin G, Too CT, et al. Differential signal transduction, membrane trafficking, and immune effector functions mediated by FcgammaRI versus FcγRIIa. Blood 2009;114:318–27.
14. Allen JM, Seed B. Isolation and expression of functional high-affinity Fc receptor complementary DNAs. Science 1989;243:378–81.
15. Bournazos S, Wang TT, Ravetch JV. The role and function of fcgamma receptors on myeloid cells. Microbiol Spectr 2016;4.
16. Bruhns P, Iannascoli B, England P, Mancardi DA, Fernandez N, Jorieux S, et al. Specificity and affinity of human Fcgamma receptors and their polymorphic variants for human IgG subclasses. Blood 2009;113:3716–25.
17. van der Heijden J, Nagelkerke S, Zhao X, Geissler J, Rispens T, van den Berg TK, et al. Haplotypes of FcγRIIa and FcγRIIIb polymorphic variants influence IgG-mediated responses in neutrophils. J Immunol 2014;192:2715–21.
18. Martner A, Aydin E, Hellstrand K. NOX2 in autoimmunity, tumor growth and metastasis. J Pathol 2019;247:151–4.
19. Hansson M, Asea A, Ersson U, Hermodsson S, Hellstrand K. Induction of apoptosis in NK cells by monocyte-derived reactive oxygen metabolites. J Immunol 1996;156:42–7.
20. Schmielau J, Finn OJ. Activated granulocytes and granulocyte-derived hydrogen peroxide are the underlying mechanism of suppression of T-cell function in advanced cancer patients. Cancer Res 2001;61:4756–60.
21. Aurelius J, Thoren FB, Akhiani AA, Brune M, Palmqvist L, Hansson M, et al. Monocytic AML cells inactivate antileukemic lymphocytes: role of NADPH oxidase/gp91(phox) expression and the PARP-1/PAR pathway of apoptosis. Blood 2012;119:5832–7.
22. Akhiani AA, Werlenius O, Aurelius J, Movitz C, Martner A, Hellstrand K, et al. Role of the ERK pathway for oxidant-induced parthanatos in human lymphocytes. PLoS One 2014;9:e89646.
23. Thoren FB, Romero AI, Hellstrand K. Oxygen radicals induce poly(ADP-ribose) polymerase-dependent cell death in cytotoxic lymphocytes. J Immunol 2006;176:7301–7.

24. Holmdahl R, Sareila O, Olsson LM, Backdahl L, Wing K. Ncf1 polymorphism reveals oxidative regulation of autoimmune chronic inflammation. Immunol Rev 2016;269:228–47.
25. Aydin E, Johansson J, Nazir FH, Hellstrand K, Martner A. Role of NOX2-derived reactive oxygen species in NK cell-mediated control of murine melanoma metastasis. Cancer Immunol Res 2017;5:804–11.
26. Billottet C, Grandage VL, Gale RE, Quattropani A, Rommel C, Vanhaesebroeck B, et al. A selective inhibitor of the p110δ isoform of PI 3-kinase inhibits AML cell proliferation and survival and increases the cytotoxic effects of VP16. Oncogene 2006;25:6648–59.
27. Chantry D, Vojtek A, Kashishian A, Holtzman DA, Wood C, Gray PW, et al. p110δ, a novel phosphatidylinositol 3-kinase catalytic subunit that associates with p85 and is expressed predominantly in leukocytes. J Biol Chem 1997;272: 19236–41.
28. Vanhaesebroeck B, Welham MJ, Kotani K, Stein R, Warne PH, Zvelebil MJ, et al. P110δ, a novel phosphoinositide 3-kinase in leukocytes. Proc Natl Acad Sci U S A 1997;94:4330–5.
29. Herman SE, Gordon AL, Wagner AJ, Heerema NA, Zhao W, Flynn JM, et al. Phosphatidylinositol 3-kinase-delta inhibitor CAL-101 shows promising preclinical activity in chronic lymphocytic leukemia by antagonizing intrinsic and extrinsic cellular survival signals. Blood 2010;116:2078–88.
30. Lannutti BJ, Meadows SA, Herman SE, Kashishian A, Steiner B, Johnson AJ, et al. CAL-101, a p110δ selective phosphatidylinositol-3-kinase inhibitor for the treatment of B-cell malignancies, inhibits PI3K signaling and cellular viability. Blood 2011;117:591–4.
31. Coutre SE, Barrientos JC, Brown JR, de Vos S, Furman RR, Keating MJ, et al. Management of adverse events associated with idelalisib treatment: expert panel opinion. Leuk Lymphoma 2015;56:2779–86.
32. Lampson BL, Kim HT, Davids MS, Abramson JS, Freedman AS, Jacobson CA, et al. Efficacy results of a phase 2 trial of first-line idelalisib plus ofatumumab in chronic lymphocytic leukemia. Blood Adv 2019;3:1167–74.
33. Zelenetz AD, Barrientos JC, Brown JR, Coiffier B, Delgado J, Egyed M, et al. Idelalisib or placebo in combination with bendamustine and rituximab in patients with relapsed or refractory chronic lymphocytic leukaemia: interim results from a phase 3, randomised, double-blind, placebo-controlled trial. Lancet Oncol 2017;18:297–311.
34. Brown JR, Byrd JC, Coutre SE, Benson DM, Flinn IW, Wagner-Johnston ND, et al. Idelalisib, an inhibitor of phosphatidylinositol 3-kinase p110δ, for relapsed/refractory chronic lymphocytic leukemia. Blood 2014;123:3390–7.
35. Furman RR, Sharman JP, Coutre SE, Cheson BD, Pagel JM, Hillmen P, et al. Idelalisib and rituximab in relapsed chronic lymphocytic leukemia. N Engl J Med 2014;370:997–1007.
36. Sharman JP, Coutre SE, Furman RR, Cheson BD, Pagel JM, Hillmen P, et al. Final results of a randomized, phase III study of rituximab with or without idelalisib followed by open-label idelalisib in patients with relapsed chronic lymphocytic leukemia. J Clin Oncol 2019;37:1391–402.
37. Condliffe AM, Davidson K, Anderson KE, Ellson CD, Crabbe T, Okkenhaug K, et al. Sequential activation of class IB and class IA PI3K is important for the primed respiratory burst of human but not murine neutrophils. Blood 2005;106: 1432–40.
38. Koyasu S. The role of PI3K in immune cells. Nat Immunol 2003;4:313–9.
39. Hoyal CR, Gutierrez A, Young BM, Catz SD, Lin JH, Tsichlis PN, et al. Modulation of p47PHOX activity by site-specific phosphorylation: Akt-dependent activation of the NADPH oxidase. Proc Natl Acad Sci U S A 2003;100:5130–5.
40. Werlenius O, Riise RE, Simpanen M, Aurelius J, Thoren FB. CD20 antibodies induce production and release of reactive oxygen species by neutrophils. Blood 2014;123:4001–2.
41. Lee H, Jung KH, Jeong Y, Hong S, Hong SS. HS-173, a novel phosphatidylinositol 3-kinase (PI3K) inhibitor, has anti-tumor activity through promoting apoptosis and inhibiting angiogenesis. Cancer Lett 2013;328:152–9.
42. Liu Y, Wan WZ, Li Y, Zhou GL, Liu XG. Recent development of ATP-competitive small molecule phosphatidylinostitol-3-kinase inhibitors as anti-cancer agents. Oncotarget 2017;8:7181–200.
43. Gharbi SI, Zvelebil MJ, Shuttleworth SJ, Hancox T, Saghir N, Timms JF, et al. Exploring the specificity of the PI3K family inhibitor LY294002. Biochem J 2007; 404:15–21.
44. Hansson M, Romero A, Thoren F, Hermodsson S, Hellstrand K. Activation of cytotoxic lymphocytes by interferon-alpha: role of oxygen radical-producing mononuclear phagocytes. J Leukoc Biol 2004;76:1207–13.
45. Day BJ. Catalase and glutathione peroxidase mimics. Biochem Pharmacol 2009; 77:285–96.
46. Shimizu Y, DeMars R. Production of human cells expressing individual transferred HLA-A,-B,-C genes using an HLA-A,-B,-C null human cell line. J Immunol 1989;142:3320–8.
47. Burkett MW, Shafer-Weaver KA, Strobl S, Baseler M, Malyguine A. A novel flow cytometric assay for evaluating cell-mediated cytotoxicity. J Immunother 2005; 28:396–402.
48. Thorén FB, Riise RE, Ousbäck J, Chiesa MD, Alsterholm M, Marcenaro E, et al. Human NK cells induce neutrophil apoptosis via an NKp46- and Fas-dependent mechanism. J Immunol 2012;188:1668–74.
49. Dahlgren C, Karlsson A. Respiratory burst in human neutrophils. J Immunol Methods 1999;232:3–14.
50. Aydin E, Hallner A, Grauers Wiktorin H, Staffas A, Hellstrand K, Martner A. NOX2 inhibition reduces oxidative stress and prolongs survival in murine KRAS induced myeloproliferative disease. Oncogene 2019;38:1534–43.
51. Thoren FB, Betten A, Romero AI, Hellstrand K. Cutting edge: antioxidative properties of myeloid dendritic cells: protection of T cells and NK cells from oxygen radical-induced inactivation and apoptosis. J Immunol 2007;179:21–5.
52. Abramoff MD, Magelhaes PJ, Ram SJ. Image processing with ImageJ. Biophotonics International 2004;11:36–42.
53. Thoren FB, Romero AI, Hermodsson S, Hellstrand K. The CD16-/CD56bright subset of NK cells is resistant to oxidant-induced cell death. J Immunol 2007;179: 781–5.
54. Alduaij W, Illidge TM. The future of anti-CD20 monoclonal antibodies: are we making progress? Blood 2011;117:2993–3001.
55. Goldstein NI, Prewett M, Zuklys K, Rockwell P, Mendelsohn J. Biological efficacy of a chimeric antibody to the epidermal growth factor receptor in a human tumor xenograft model. Clin Cancer Res 1995;1:1311–8.
56. Park JW, Hoyal CR, Benna JE, Babior BM. Kinase-dependent activation of the leukocyte NADPH oxidase in a cell-free system. Phosphorylation of membranes and p47(PHOX) during oxidase activation. J Biol Chem 1997; 272:11035–43.
57. Babior BM. NADPH oxidase: an update. Blood 1999;93:1464–76.
58. Sekhsaria S, Gallin JI, Linton GF, Mallory RM, Mulligan RC, Malech HL. Peripheral blood progenitors as a target for genetic correction of p47phox-deficient chronic granulomatous disease. Proc Natl Acad Sci U S A 1993;90: 7446–50.
59. El Benna J, Faust RP, Johnson JL, Babior BM. Phosphorylation of the respiratory burst oxidase subunit p47phox as determined by two-dimensional phosphopeptide mapping. Phosphorylation by protein kinase C, protein kinase A, and a mitogen-activated protein kinase. J Biol Chem 1996;271:6374–8.
60. Nauseef WM, Volpp BD, McCormick S, Leidal KG, Clark RA. Assembly of the neutrophil respiratory burst oxidase. Protein kinase C promotes cytoskeletal and membrane association of cytosolic oxidase components. J Biol Chem 1991;266: 5911–7.
61. Ding J, Vlahos CJ, Liu R, Brown RF, Badwey JA. Antagonists of phosphatidylinositol 3-kinase block activation of several novel protein kinases in neutrophils. J Biol Chem 1995;270:11684–91.
62. Didichenko SA, Tilton B, Hemmings BA, Ballmer-Hofer K, Thelen M. Constitutive activation of protein kinase B and phosphorylation of p47phox by a membrane-targeted phosphoinositide 3-kinase. Curr Biol 1996;6:1271–8.
63. Hansson M, Hermodsson S, Brune M, Mellqvist UH, Naredi P, Betten A, et al. Histamine protects T cells and natural killer cells against oxidative stress. J Interferon Cytokine Res 1999;19:1135–44.
64. Dong S, Harrington BK, Hu EY, Greene JT, Lehman AM, Tran M, et al. PI3K p110δ inactivation antagonizes chronic lymphocytic leukemia and reverses T cell immune suppression. J Clin Invest 2019;129:122–36.
65. Aurelius J, Martner A, Brune M, Palmqvist L, Hansson M, Hellstrand K, et al. Remission maintenance in acute myeloid leukemia: impact of functional histamine H2 receptors expressed by leukemic cells. Haematologica 2012;97:1904–8.
66. Ali K, Soond DR, Pineiro R, Hagemann T, Pearce W, Lim EL, et al. Inactivation of PI(3)K p110δ breaks regulatory T-cell-mediated immune tolerance to cancer. Nature 2014;510:407–11.